

Realization and Characterization of an Electronic Instrument Transducer for MV Networks with Fiber Optic Insulation

DANIELE GALLO⁽¹⁾, CARMINE LANDI⁽¹⁾, MARIO LUISO⁽¹⁾
EDOARDO FIORUCCI⁽²⁾, GIOVANNI BUCCI⁽²⁾, FABRIZIO CIANCETTA⁽²⁾

⁽¹⁾ Department of Information Engineering
Second University of Naples
Via Roma 29 - 81031 Aversa (CE),
ITALY
{daniele.gallo, carmine.landi, mario.luiso}@unina2.it <http://www.unina2.it>

⁽²⁾ Department of Electrical and Information Engineering
University of L'Aquila
Via G. Gronchi 18 – Pile, 67100 L'Aquila
ITALY
{giovanni.bucci, edoardo.fiorucci, fabrizio.ciancetta}@univaq.it <http://www.univaq.it>

Abstract: - As a consequence of increasing interest in power quality analysis, the measuring instruments used in electrical power systems are now charged with new tasks to be undertaken for which the equipment already installed or traditionally used are very unlikely to be adequate. Particular problems come from the first part of each electrical measurement chain: voltage and current transducer are profitably usable only in a narrow 50-400 Hz frequency range while for power quality analysis a much larger frequency range should be analyzable. This paper presents a voltage transducer prototype designed to be installed in medium voltage systems. The presented design criteria try to face both the bandwidth limitations and the accuracy problems that characterize commercial transducers commonly adopted. In addition, the presented implementation keeps the galvanic insulation characteristic, that is mandatory for this kind of equipment. Commercial components are used in the presented prototype to keep the budgetary requirement low. Some results of prototype characterization are presented in the last part of the paper.

Key-Words: - voltage transducer, voltage measurement, medium voltage, power quality

1 Introduction

Globally electric utilities, but especially in Europe, are heavily investing to upgrade their antiquated delivery, pricing, and service networks including investments in different areas such as advanced metering infrastructure, which usually includes control and monitoring of devices and appliances inside customer premises. In this context, Power Quality (PQ) aspects have recently become a pressing concern in electrical power systems due to the increasing number of perturbing loads and the susceptibility of loads to power quality problems. Obviously, electrical disturbances can have significant economic consequences for customers, but they can also have serious economic impacts on the utility companies, because the new, liberalized competitive markets allow customers the flexibility

of choosing which utility serves them. In practice, the new, liberalized markets throughout the world are changing the framework in which power quality is addressed and power quality objectives are now of great importance to all power system operators [1].

As a consequence, the measuring instruments used in electrical power systems are now charged with new tasks to be undertaken for which the equipment already installed or used traditionally are very unlikely to be adequate. Particular problems come from the first part of measurement chain: voltage and current transducer (VT and CT). This paper is particularly interested in the voltage transducers, anyway some design and implementation considerations presented in the following could be extended to current transducers

with minor changes taking into accounts their substantial differences. The commercial voltage transducers that are most widely installed in power systems are based on transformers.

The evaluation of the precision class of MV inductive voltage transformers (IVT's) have been discussed and investigated in the past in papers as [2], that is focused on their verification in the field, using the results obtained in the usual tests of no-load loss, short circuit current and winding ohmic resistances, performed with common instruments. Using the Mollinger & Gewecke [3] diagram together with the results of an accuracy measurements on some commercial IVT's, the exact value of the winding turns and the primary winding dispersion reactance have been evaluated, to calculate phase and magnitude errors. The errors were compared with the ones obtained with the Shering-Alberti method. An innovative approach for the modelling of inductive voltage transformers (IVT's) has been proposed in [4], leading to an analysis of the instrument transformer that is independent by the waveform shape of the voltage applied to its primary winding and simply based on the measurement of the input and output signals. The authors propose an experimental procedure for the identification of the model parameters of an IVT's at the AC-mains frequency.

The performance and the frequency response of MV voltage transformers have been recently investigated by authors that focused on different characterization issues [5, 6, 7]; it is known that the standard [8] for IVT's does not define accuracy limits for frequency other than the rated frequency, so IEC TC38/AHG41 has started working on a technical document covering the accuracy of instruments transformers for power quality measurements, including harmonics. In [5] a systematic analysis on how the accuracy of IVT's depends on the frequency of the voltage harmonics has been performed, introducing a list of factors of influence on the IVT frequency response is presented, and a measuring methodology based on the FFT algorithm; some MV voltage with cast resin insulation are tested, by considering the feeding directions, different amplitudes of the test signals, the manufacturing tolerances and the type design tolerances, the burden values and the operating temperature. The results in [5] show that the frequency range for acceptable accuracy of IVT's is limited for harmonic measurements; for measurements in the frequency range between 2 kHz and 9 kHz the accuracy of the adopted IVT's should be carefully verified because of the complex system of influence factors having effects on it.

In [6], after performing some experimental tests on IVT's, the authors propose and validate some lumped elements models describing the IVT's behaviour for frequencies up to 5 kHz.

The comparison between the performances of optical voltage transformers (OVT) and IVT's have been performed by the authors of [7]; a particular attention has been given to the performance for transient phenomena as the lightning impulses, and equivalent circuits proposed for both OVT and IVT.

This kind of voltage transducer are profitably usable only in a narrow 50-400 Hz frequency range while for power quality analysis a much larger frequency range should be analyzable. In fact, those limits make them unusable for some of main PQ analyses such as harmonic analysis but also for more sophisticated analysis at low frequencies such as subharmonic analysis. In order to overcome these limits, different kinds of voltage and current transducers have been developed, [1]-[12]: they have been designed to enlarge the analyzed frequency range and at the same time to keep good accuracy. Nevertheless, in most cases they have got high costs too that obviously prevent their wide spreading. Authors have already presented voltage transducers with wide bandwidth for Low Voltage (LV) electrical system [13]-[15]; this paper presents a new design of transducer that improves the performance of preceding transducers and it is specifically designed for Medium Voltage (MV) system. It was firstly described in [16], but here more complete descriptions of operation, design, simulations, realization and characterization are discussed. It was designed with the aim of facing both the bandwidth limitations and the accuracy problems that are briefly previously recalled. In addition, the presented implementation keeps the galvanic insulation characteristic, that is mandatory for this kind of equipment, with the adoption of signal transmission through an optical fiber. Commercial components are used in the prototype to keep the budgetary requirement low.

The paper in the following is organized in a way that section II deals with transducer design criteria; the other sections, from the III to the VI, respectively, present the design, the simulations, the realization and the characterization of the realized voltage transducer (RVT).

2 Design Criteria

2.1 Input range and bandwidth

The design of a voltage transducer, intended for power quality measurements, must begin from the

analysis of the international standards [17]-[22]. From the analysis of [18] it is evident that the most strict uncertainty level is established for the assessment of the root mean square (r.m.s.) value of the supply voltage, which has to be measured with accuracy of $\pm 0.1\%$. Moreover, in [22], which deals with compatibility levels in industrial plants for low-frequency conducted disturbances, limits for voltage components up to 9 kHz are established. It has not to be ignored that this limit is increasing year after year, due to advance in power electronics and switching devices. A requirement comes once more from [18]: voltage transducers should be sized to prevent measured disturbances from inducing saturation. This requires that the knee point of the transducer saturation curve be at least 200% of the nominal system voltage. All these considerations results in the following design specifications: a voltage transducer must have accuracy of $\pm 0.1\%$, a -3 dB frequency bandwidth equal at least to 9 kHz and its full scale range must be at least 200% of the nominal system voltage. The RVT has been designed accounting these requirements on accuracy, frequency bandwidth and input full scale range.

2.1 Input range and bandwidth

The core of the RVT is the optical insulation stage. As it is well known ([22]), an optical transmitter has a non-linear current/light power characteristic. This fact has forced to use, in power system applications, an optical link as a mean to obtain galvanic insulation only as a digital communication channel. In fact, since a digital communication, either serial or parallel, is composed of a sequence of pulses and the information is only linked to a low or high level of such pulses, even if the channel produces a distortion in the transmitted waveform, the information is preserved. The most important parameter of a digital optical communication channel is the response time, which is in turn inversely proportional to frequency bandwidth: the lower is the response time, the wider is the frequency bandwidth and thus the higher is the baud rate of the channel.

On the contrary, in an analog optical communication channel, since the information is linked to the shape of the transmitted waveform, the distortion must be as low as possible.

The basic idea at the base of this paper comes from control system theory: if a non-linear system is utilized around a working point in a quite linear portion of its characteristic and inserted in a feedback loop control scheme, it can be considered a linear system [23].

A simplified block scheme of an open loop optical link is shown in Figure 1. For the case in question, the non linear system is the optical transmitter (OT_1): if it is coupled to an optical receiver (OR_1), through a fiber optic, the relationship among input and output currents, respectively I_{IIN} and I_{IOUT} , is not linear, since the relationship among input current and transmitted light power (L_1) is not linear.

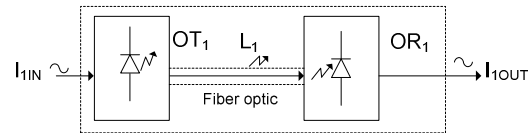


Fig.1 - Block scheme of the open loop optical link

Anyway, if another couple of one OR and one OT, matched with the first couple, is used in a feedback loop control scheme as in Figure 2, its role becomes crucial. In fact, since the two couples OT_1 - OR_1 and OT_2 - OR_2 share the same input current (I_{IIN} is equal to I_{2IN}) the output current I_{2OUT} is a reproduction of the output current I_{IOUT} of the first couple: thus I_{2OUT} can be used to modify the current I_{IIN} in OT_1 in order to have a linear relationship among the global output current (I_{OUT} , which is equal to I_{IOUT}) and input current (I_{REF}), using a proper signal conditioning (the block "COND" in Figure 2).

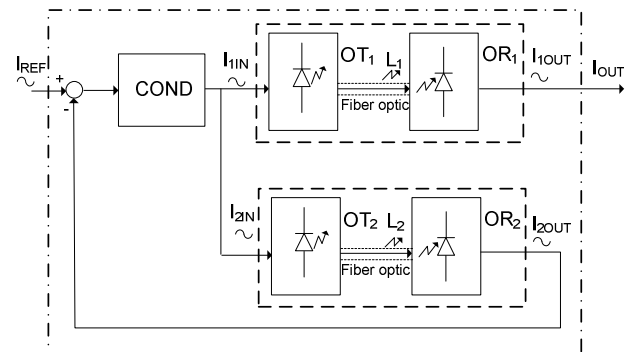


Fig. 2 - Block scheme of the closed loop optical link

It is worthwhile underlining the vital importance of the matching between the two OR: the better the matching is, the more effective the linearization will be. In the next section the design of the optical link and, in general, that of the entire transducer is shown.

3 Transducer Design

The architecture of the RVT is divided in three sections: the first one is the input stage which

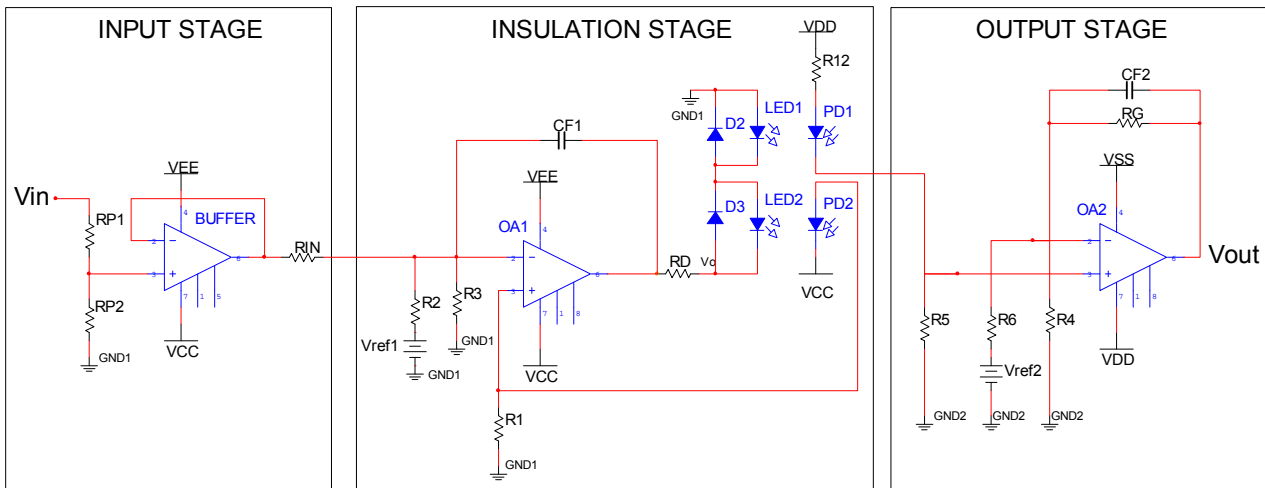


Fig. 4 - Simplified circuital scheme of the transducer.

couples the transducer to the voltage source, having an high input impedance; the second one is the optical insulation stage, which separate low voltage output section from high voltage input section; finally, the third one is the output stage which couples the transducer with the input stage of measuring instruments. Block scheme of the RVT is shown in Figure 3. The functional block diagram of insulation stage, as it is explained in the previous section, is shown in Figure 2. The simplified circuital scheme of the RVT is shown in Figure 4. The same three stages of Figure 3 can be found. The descriptions of such stages are in the following subsections.

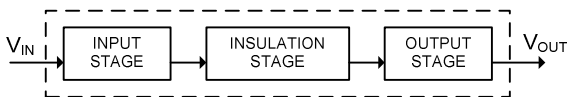


Fig.3 - Block scheme of realized voltage transducer

3.1 Input stage

The input stage is the most critical part of the entire circuit: in fact, since it is directly connected to voltage source, it manages the highest voltage values. In [17] a medium voltage network is defined as an electrical network with a nominal voltage in the range of 1000 V ÷ 30000 V. Thus, according to [18] a voltage transducer for MV networks must have an input range at least of $\pm 60000 \cdot \sqrt{2}$ V, which corresponds to about ± 85000 V. As it is well known the dielectric rigidity of dry air is about 3000 V/mm. So, in order to avoid the generation of an electric arc between RVT terminals, such a requirement on distance must be taken into account: in particular, since air is not dry in real operating conditions it has been considered that actual air

dielectric rigidity is 300 V/mm, that is one tenth of dry air rigidity. The input stage of the RVT is a resistive voltage divider with an operational amplifier for impedance adaptation. Its simplified circuital scheme is shown in inset “INPUT STAGE” of Figure 4. For design specification, the output of op-amp BUFFER is in the range of ± 5 V. Design criteria for resistances RP1 and RP2 are: 1) the voltage divider must realize an attenuation of about 17000; 2) the maximum power dissipated on RP1 and RP2 must be equal to 1 W. The first criterion comes from the ratio 85000/5 V/V, which are respectively, input and output voltage; the second criterion comes from the fact that the lower is the power dissipated by a resistor the lower are its cost and the load effect on the network. In mathematical terms, such criteria are:

$$\begin{cases} \frac{RP2}{RP1 + RP2} = \frac{1}{17000} \\ \frac{60000^2}{RP1 + RP2} = 1 \end{cases} \quad (1)$$

From equations in (1) it results RP2 equal to about 212 kΩ and RP1 equal to about 3.6 GΩ. Such resistances have been realized with commercially available non-inductive thick film resistors: RP1 is realized with a series of seven resistors having resistance equal to 500 MΩ, RP2 is realized with a resistor having resistance equal to 200 kΩ. Thus, RP1 is equal to 3.5 GΩ and RP2 is equal to 200 kΩ. All the resistors have maximum power equal to 1.5 W. With such values, the attenuation of voltage divider is about 17500, and the dissipated power is about 1.03 W. The current in the voltage divider is about 17 μA: voltage drop across 500 MΩ resistors is about 8570 V. Each resistor is about 27.4 mm

long: it results in a value of voltage per millimeter equal to 312.8 V/mm. Such a value is a bit higher than that of specification, i.e. 300 V/mm; anyway it must be considered that in nominal operating conditions, with system voltage equal to 30000 V, this value is about 156 V/mm. Voltage drop across 200 k Ω resistor is 3.42 V at the most. Op-amp BUFFER is utilized in voltage buffer configuration: it has voltage supply of ± 12 V, distortion of 0.0035 % at 10 kHz, -3 dB bandwidth of 12 MHz, slew rate of 30 V/ μ s, short circuit output current of 20 mA, differential input resistance of 10^{13} Ω , output resistance of 40 Ω . Particularly the high value of input resistance is very important, in order not to influence the operation of voltage divider which has a high resistance. Totally, with input voltage of ± 85000 V, the output of the operational amplifier BUFFER is about ± 4.86 V. As it is indicated in Figure 4 and in Figure 2, the input of insulation stage is a reference current (I_{REF} in Figure 2): in order to produce such a reference current from the output of BUFFER, a resistance R_{IN} is inserted at output terminal of BUFFER. In this way with output voltage of ± 4.86 V it produces a current of about ± 225 μ A.

3.2 Insulation stage

As it has been said in the beginning of this section, the insulation stage realizes the galvanic insulation between the voltage source (i.e. the network operating at medium voltage level) and the measuring instrument (operating at ± 5 V level). Moreover, as it is described in section II, the galvanic insulation is obtained through a double conversion, electrical-to-optical and optical-to-electrical, of the signals in the circuit. The simplified electrical scheme is shown in inset "INPUT STAGE" of Figure 4. The electrical-to-optical conversion is performed by an infrared light emitting diode (LED1) and the optical-to-electrical conversion is performed by an infrared photodiode (PD1) they are coupled through a plastic optical fiber (POF). The task of LED1 and PD1 is described in section II: LED1 has the role of OT1 and PD1 has the role of OR1. They are used in a closed loop circuit scheme, like in Figure 2, together with another couple of light emitting diode and photodiode: LED2 and PD2 in Figure 4 have the roles, respectively, of OT2 and OR2 in Figure 2. It is worthwhile noting that also LED2 and PD2 are coupled through a POF.

The two utilized LEDs have the same nominal specifications: they have a plastic package and a micro lens which allows an efficient coupling with a POF with core of 1000 μ m. Their main

characteristics are: peak wavelength (maximum of optical power) equal to 870 nm, spectral bandwidth (at 50 % of maximum current) of 30 nm, optical power transmitted on fiber (at 50 % of maximum current) of 300 μ W, rise and fall times (10 % to 90 % and 90 % to 10 %) of 3.0 ns, capacity (at 1 MHz) of 120 pF, direct voltage (at current of 20 mA) of 1.85 V. In order to maximize optical power coupling between transmitter and receiver, the utilized PDs, which in turn have the same nominal specifications, have optical bandwidth compatible with LEDs. Like the LEDs, they have a plastic package and a micro lens which allows an efficient coupling with a POF. Their main characteristics are: peak wavelength (maximum of optical power) equal to 880 nm, spectral bandwidth (at 10 % of maximum input power) in the range of 400÷1000 nm, rise and fall times (10 % to 90 % and 90 % to 10 %) of 3.0 ns, capacity (at 1 MHz) of 4 pF, direct voltage of 1.2 V, responsivity equal to 0.2 μ A/ μ W at wavelength of 632 nm and to 0.4 μ A/ μ W at wavelength of 880 nm.

As it has been said before, as optical fiber a POF has been used, in order to make LEDs and PDs work properly; it has some characteristics that differentiate it from classical fibers. Its core diameter is 980 μ m against 8 – 62.5 μ m of classical fibers; thus, thanks to core dimension, a POF does not require to be perfectly aligned with LEDs and PDs and it works properly also in the case of strong vibrations. Moreover it does not oxidize and it does not get damaged in the presence of rain. All these characteristics makes it preferable to work in harsh environments like MV/LV transformation stations.

The task of realization of closed loop scheme is performed through the use of the operational amplifier OA1, shown in Figure 4. Main specifications of OA1 are: it has voltage supply of ± 12 V, -3 dB bandwidth of 1 GHz, slew rate of 400 V/ μ s, short circuit output current of 60 mA, differential input resistance of 15 k Ω , output resistance of 3 Ω .

Such op-amp has been preferred over the op-amp in the input stage, i.e. BUFFER, thanks to its much higher gain-bandwidth product, which allows to improve optical feedback enlarging transducer overall bandwidth, and its low input resistance, which allows to reduce influence of parasitic components. The aim of OA1 is to give the two LEDs a current proportional to input current. Particularly from the simplified circuit scheme in Figure 4, it can be seen that the two LEDs are in series: in such a way they share the same current. Also the parallel connection assures the same current, imposing the same voltage drop: anyway

this connection requires a higher output current from OA1.

This op-amp has a double feedback, in order to generate an higher amplification of LEDs current. Since LEDs work only with a unipolar current, the bipolar input current is summed to a constant unipolar reference current, obtained from a constant unipolar voltage reference (V_{ref1} in Figure 4), realized through a zener diode, polarized with a resistance: the zener diode has a capacitor in parallel, in order to stabilize the voltage and thus to reduce disturbances.

With the hypothesis that the LEDs, the PDs and the lengths of the two fibers are perfectly equal by twos, the feedback current (i.e. the current in PD2) is exactly the same of the insulation stage output current (i.e. the current in PD1). It is important that such hypothesis is at best verified in order to make the LEDs and the PDs work in the same point of transfer characteristics and thus to compensate non-linearities.

Totally, with an input current of about $\pm 225 \mu\text{A}$ (i.e. peak-to-peak amplitude of about $450 \mu\text{A}$), the output current of insulation stage has peak-to-peak amplitude of about $45 \mu\text{A}$: anyway it has a non zero mean value, since it has to be a unipolar current.

3.3 Output stage

The output stage couples the transducer with the input stage of measuring instruments: its main tasks are 1) the final proper conditioning which makes the signal suitable for measuring instruments, 2) impedance adaptation, 3) bandwidth limitation and 4) noise rejection. It converts the output current of PD1 in a voltage, which is the output signal of the entire circuit. The same op-amp and voltage reference of those in insulation stage have been used.

Employing the same operation principle of the insulation stage, the output stage is composed by a single stadium of operational amplifiers, thanks to a double amplification of current. In fact, since the current in PD1 is in the microamperes range, in order to obtain an output voltage in the range of volts with a single amplification gain in the range of 10^6 and thus resistances in the range of megaohm should be used. Nevertheless, such resistances value are comparable with input resistance of OA2 and this makes the hypothesis of infinite input resistance fail.

Resistive trimmers are also used for gain and offset regulation. Thanks to voltage reference V_{ref2} , the unipolar current in PD1 is converted to a bipolar voltage.

Considering the whole transducer, with an input voltage of $\pm 85000 \text{ V}$, the output is $\pm 5 \text{ V}$.

3.4 Power Supply

Power supply of the various stages of the circuit have been obtained by means of $+12 \text{ V}/\pm 12 \text{ V}$ isolated DC/DC converters: one for input and transmission stage, one for reception stage, in order to have galvanic separation between grounds. The power supply of the DC/DC converters could be taken from input voltage; anyway, in order to preserve transducer operation in the case of voltage dips and interruptions, which are power quality phenomena that RVT must measure, another solution has been utilized. Power supply has been obtained from a 12 V , 3 W photovoltaic panel, with a 12 V , 7 ampere-hour battery in parallel; in order to avoid current circulation from battery to panel, a diode has been inserted with anode connected to positive terminal of panel and cathode connected to positive terminal of battery. In the case of an interruption, considering RVT power consumption, with such a battery the operation is assured at least for three days.

4 Transducer Simulation

The design of the proposed voltage transducer has passed through the execution of several simulations. The aim of simulation is to find the best values of resistors and capacitors that optimize circuit performance. The RVT has been simulated in Multisim environment. SPICE models for the electronic components have been used, taking them from manufacturer datasheet. Regarding the SPICE models of LEDs and PDs, they are not enclosed in manufacturer datasheet: therefore standard models of LEDs and PDs, contained in simulation environment, have been used, customizing them for the case at hand using the information enclosed in components datasheets. The only parameter which has been measured, here named α , is the parameter that takes into account the fiber attenuation and the losses between LEDs and fibers and between fibers and PDs.

Neglecting the effect of parasitic resistance, such parameter can be estimated through a direct polarization of LEDs with a direct current (DC), measuring the currents in the LEDs (I_{LED}) and the PDs (I_{PD}). The values of α for fiber lengths of 5 m (α_5) and 1 m (α_1) are respectively as follows:

$$\alpha_5 = \frac{I_{PD}}{I_{LED}} = 0.000113 \quad (2)$$

$$\alpha_1 = \frac{I_{PD}}{I_{LED}} = 0.00280 \quad (3)$$

For the two couples of LEDs and PDs the parameters α_5 and α_7 have the same values. In order to prove the effectiveness of the closed loop scheme, simulations relating open loop configuration and closed loop configuration are reported.

First of all, time domain analysis has been performed: in Multisim environment it is called “Transient Analysis”. In Figure 5 and Figure 6 the input and the output signals of, respectively, open loop and closed loop transducers are shown. The input has an amplitude of 85000 V and frequency of 50 Hz: the outputs of both transducers have amplitudes of 5 V.

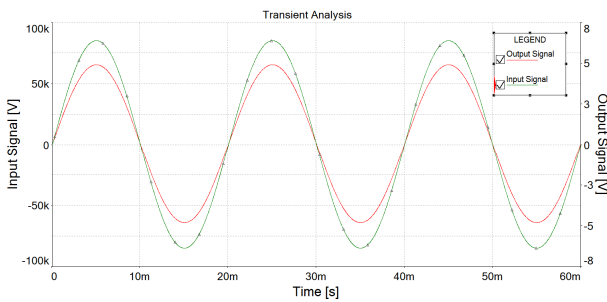


Fig. 5 – Time domain analysis for open loop transducer.

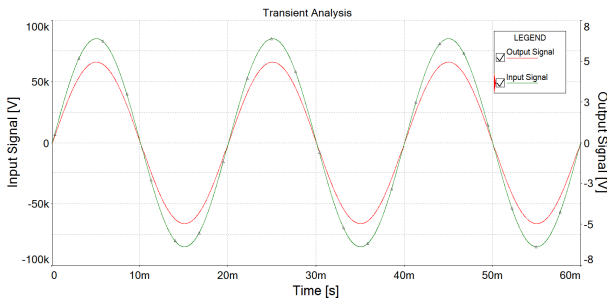


Fig. 6 - Time domain analysis for closed loop transducer

Then, in order to test the distortion introduced by the RVT, a spectral analysis, which is called “Fourier Analysis” in Multisim environment, has been performed. Both the open loop and closed loop transducers are supplied with a sinusoidal signal having amplitude of 85000 V and frequency of 50 Hz. The Fast Fourier Transform (FFT) has been executed on input and output signals: for sake of clarity only the first 200 harmonic components have been considered. In Figure 7 the normalized magnitude spectrum of input signal is shown: it can

be seen that the higher harmonic amplitude value, due only to numerical approximations, is lower than 10^{-7} (i.e. more than seven magnitude orders lower) and the Total Harmonic Distortion (THD) is equal to 9.02e-6 %. In Figure 8 the normalized magnitude spectrum of output signal of open loop transducer is shown: it can be seen that it introduces a second order harmonic (i.e. at frequency of 100 Hz) with a high amplitude, about 10^{-3} , that is three magnitude orders lower.

Totally the THD is 0.133 %. But then the presence of high harmonic amplitude values are the effect of a non-linearity, which is present in the circuit, as it is said in section II, and it is due to the non linear electrical-to-optical and optical-to-electrical conversions performed respectively by the LED and the PD.

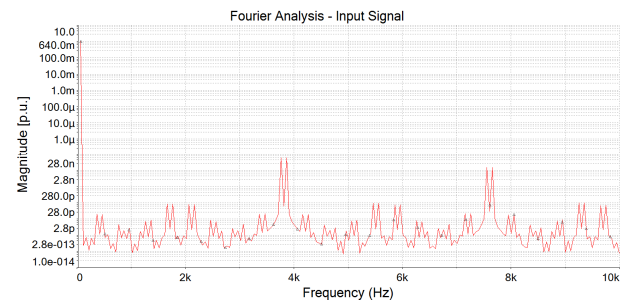


Fig. 7 - Normalized magnitude spectrum of transducer input signal.

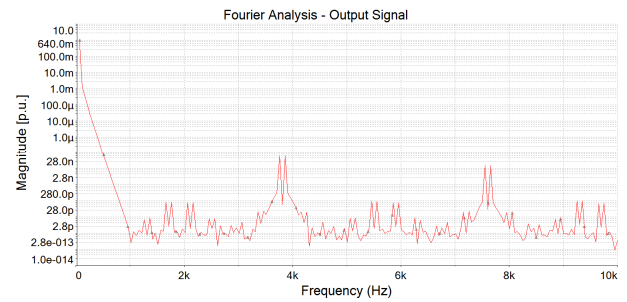


Fig. 8 - Normalized magnitude spectrum of output of open loop transducer.

In Figure 9 the normalized magnitude spectrum of output signal of closed loop transducer is shown: it can be seen that the higher harmonic amplitude value is that of second order harmonic which is about 10^{-6} , i.e. about six magnitude orders lower. Totally the THD is 0.000217 %, that is about three magnitude orders lower than THD introduced by open loop transducer. This means that the proposed closed loop scheme realizes a very effective linearization of the non linear optical LED-PD system.

The last analysis here reported regards the frequency response. In Multisim environment the “AC Analysis” has been performed. In Figure 10 and Figure 11, respectively, the magnitude and the phase frequency responses of the open loop transducer are shown, while in Figure 12 and Figure 13, respectively, the magnitude and the phase frequency responses of the open loop transducer are shown.

From them it can be seen that both the transducers introduce an attenuation of 17000, as it comes from the design in section III: moreover the -3 dB bandwidth is 2.37 MHz for open loop transducer and 2.33 MHz for closed loop transducer. At the -3 dB frequency point, phase response is -78.1 degrees for open loop transducer and -88.8 degrees for closed loop transducer.

From simulations it results that closed loop transducer introduces a little bit higher delay in the phase response.

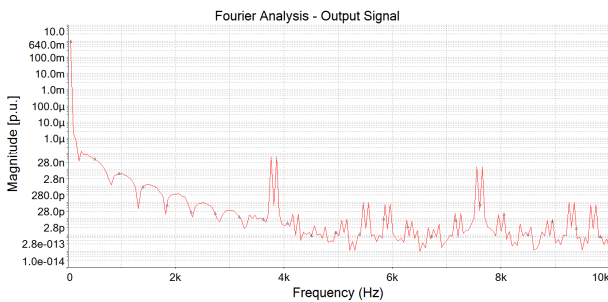


Fig. 9 - Normalized magnitude spectrum of output of closed loop transducer.

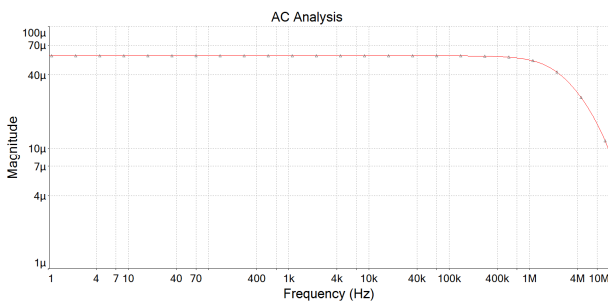


Fig. 10 – Magnitude frequency response of open loop transducer.

Anyway, the magnitude responses related to the two transducer configurations are practically the same and, above all, the closed loop configuration makes the RVT an effective linear voltage transducer. Moreover, from simulations it follows that RVT performance are much better than that prescribed in [17], [22], [15] and summarized in section II.

5 Transducer realization

The design and the simulation of the proposed voltage transducer have led to find the best nominal value for resistances and capacitances in order to obtain the best performance.

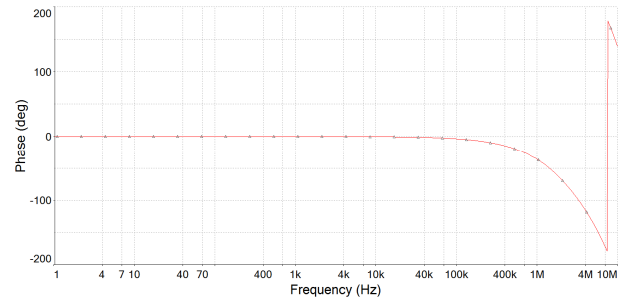


Fig. 11 - Phase frequency response of open loop transducer.

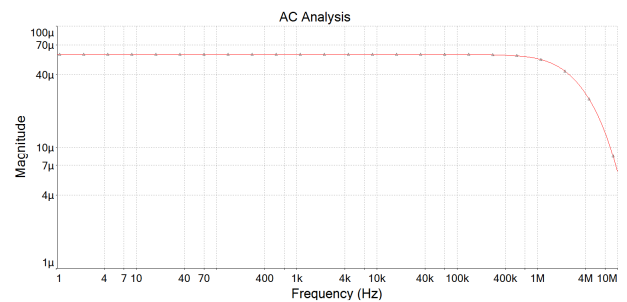


Fig. 12 - Magnitude frequency response of closed loop transducer.

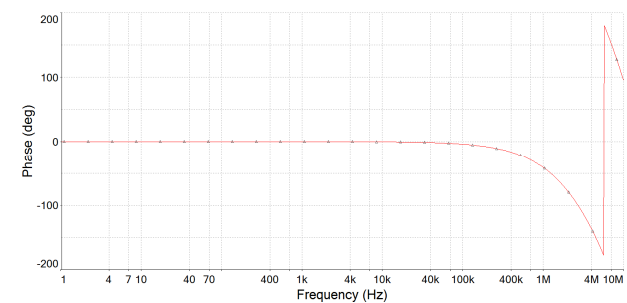


Fig. 13 - Phase frequency response of closed loop transducer.

In the phase of realization, anyway, commercially available resistors and capacitors have been used and they are affected by a tolerance and parasitic effects: these makes the actual RVT performance deviate from the simulated performance. Especially the resistors of the voltage divider in the input stage of the RVT influence the rated ratio of the entire RVT. The prototype of the RVT is physically divided in three parts: the voltage divider alone, the

transmission board which contains the remaining part of the input stage and the entire insulation stage without the photodiode PD1 and finally the reception board which contains PD1 and the entire output stage. The photos of the voltage divider, transmission board and reception board are shown, respectively, in Figure 14, Figure 15 and Figure 16. The voltage divider and the transmission board are linked through an electrical connection, while the transmission and the reception boards are connected through a plastic optical fiber.



Fig. 14 - Photo of the voltage divider of the RVT.

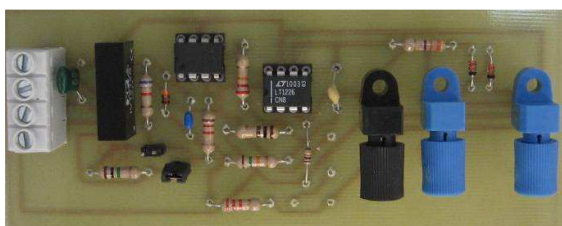


Fig. 15 - Photo of the transmission board of the RVT.

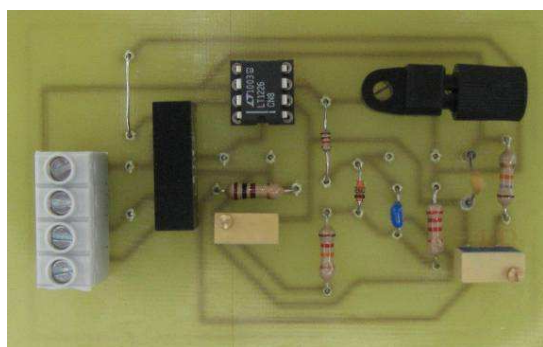


Fig. 16 - Photo of the reception board of the RVT.

6 Transducer characterization

The characterization of a voltage transducer for medium voltage network, intended to be used for analysis of quality of voltage supply, presents some specific issues, related to the fact that, at best author

knowledge at the time this paper is written, a test system for a full characterization, from a PQ point of view, of voltage transducers for MV networks are not commercially available.

Therefore the characterization of the RVT has been performed in various steps and they are described in the next subsections.

6.1 Tests at rated frequency

In the first group of tests the ratio error and phase displacement, at rated frequency (i.e. 50 Hz) and 80 %, 100 % and 120 % of rated voltage (i.e. 30 kV) have been tested. These tests have been executed through an industrial system for automated calibration of voltage and current measurement transformers for MV networks. Such a machine has been developed by a company based in a town near Aversa (CE), Italy, the city of the Second University of Naples. Main specifications of such a system are in the Table 1.

The RVT has been compared with a standard Voltage measurement Transformer (VT), with rated primary voltage of 30000 V_{RMS} and accuracy class of 0.1. The rated ratio of the RVT has been measured and it is 17000. It is worth noting that ratio and offset of the RVT can be adjusted through trimmers in the output stage. Ratio errors and phase displacements resulting from the first group of tests are summarized in Table 2.

From Table 2 it can be seen that the ratio error is contained in the range of $\pm 0.02\%$: therefore it can be given the 0.1 accuracy class.

6.2 Frequency response

The second group of tests regards the frequency response of the RVT. In this group of tests the voltage divider in the input stage of the RVT and the rest of the RVT have been characterized separately.

Regarding the voltage divider, its impedance has been characterized with the numeric impedance meter Schlumberger SI 1260, in the frequency range of 20 Hz \div 100 kHz. The magnitude response is shown in Figure 17. It can be seen that attenuation at 50 Hz is about 17390; moreover it introduces a deviation of about 5 % at 100 kHz.

The RVT without the voltage divider has been characterized through a measurement station based on PXI platform, with a ± 10 V, 14 bits, 2.5 MHz data acquisition board and with a ± 12 V, 16 bits, 100 MHz arbitrary waveform generator. Sinusoidal signals, in the range of 10 Hz \div 100 kHz, with amplitude of 5 V have been generated. Figure 18 shows the magnitude response of the RVT, while Figure 19 shows the phase response of the RVT: magnitude response is in the range of $\pm 0.05\%$ until

100 kHz, while phase response is lower than 50 mrad at 100 kHz. From characterization it follows that RVT performance is much better than that prescribed in [17]-[22] and summarized in section II: in fact it has an accuracy class of 0.1, its full scale range is over 200 % of the maximum medium voltage amplitude level (i.e. 30 kV_{RMS}, [17]) and its frequency bandwidth exceeds 100 kHz.

TABLE 1. Main specifications of voltage measurement transformers automated calibration system

Quantity	Range	Resolution	Accuracy
Test Frequency	40 – 100 Hz	0.1 Hz	±(1%+3dgt)
Generator supply current	0 – 50 A _{RMS}	0.1 A	±(1%+3dgt)
Voltage on burden	0 – 200 V _{RMS}	0.1 V	±(1%+3dgt)
Test voltage	0 – 60 kV _{RMS}	0.01 kV	±(1%+3dgt)
Resistance	0.020 – 15 Ω 20 – 19000 Ω	0.001 Ω 1 Ω	±(0.5%+3dgt)
Ratio error	± 0.1 % - ± 6 %	0.01 %	±(1%+3dgt)
Phase displacement	± 1.5 mrad - ± 70 mrad	0.1 mrad	±(1%+3dgt)
Current on burden	0 – 10 A _{RMS}	0.001 A	±(1%+3dgt)
Partial discharge	0 – 10 pC 0 – 100 pC 0 – 1000 pC	0.1 pC 1 pC 10 pC	±(2%+5dgt)
Environment Temperature	283 – 313 K	0.1 K	± 1 K
Burden	1 – 200 VA	0.125 VA	±(5%+3dgt)
Standard	3000/100 V/V 30000/100 V/V		0.1 accuracy class

TABLE 2. Results of tests on realized voltage transducer at rated frequency

	Test Voltage [% of rated voltage]		
	80	100	120
Ratio error [%]	-0.02	0.02	-0.01
Phase displacement [mrad]	0.1	0.1	0.1

7 Conclusion

In this paper the realization and the characterization of an electronic instrument transducer for medium voltage networks with fiber optic insulation is presented. Design criteria for the transducer, its design, simulation and experimental characterization are shown.

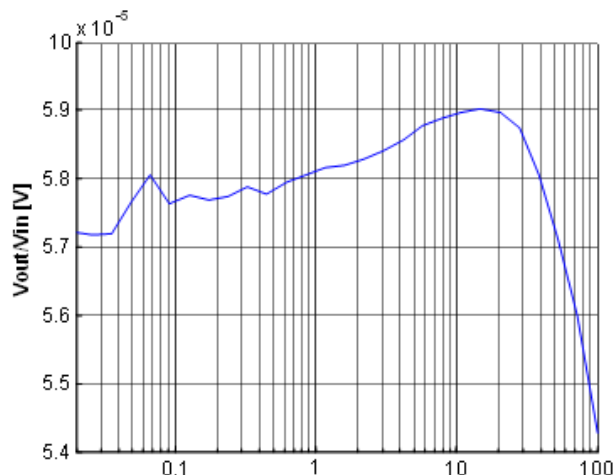


Fig. 17 - Magnitude response of the voltage divider

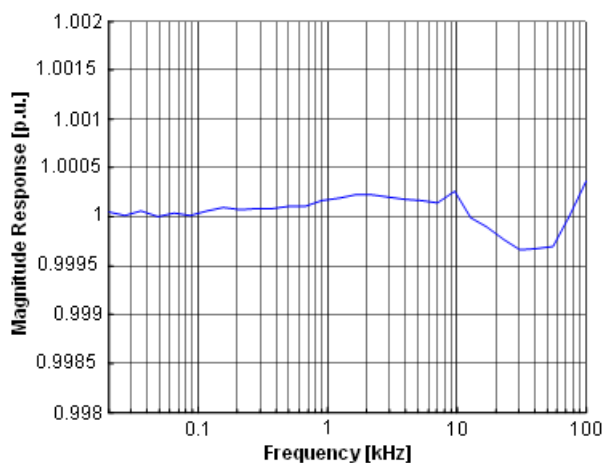


Fig. 18 - Magnitude response of RVT without voltage divider.

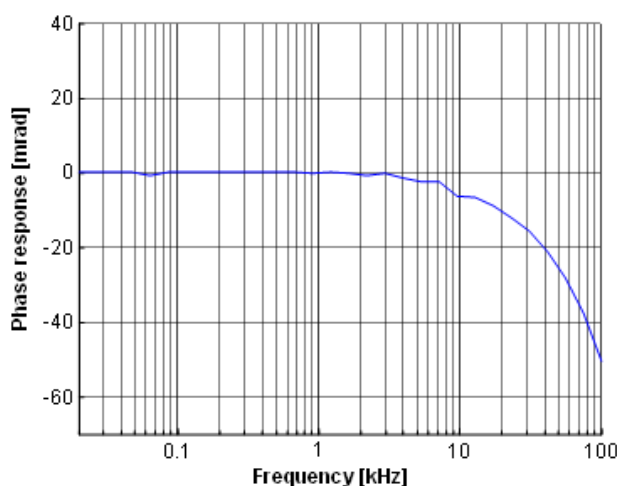


Fig. 19 - Phase response of RVT without voltage divider.

From experimental results it can be seen that RVT exhibits accuracy and bandwidth that are better than those prescribed by international standards on power quality measurements. Moreover, it is composed of simple electric and electronic components: so it has a low cost. Its features makes it attractive for a large scale utilization in the new smart grid scenario.

References:

- [1] P. Caramia, G. Carpinelli, P. Verde "Quality Indices in Liberalized Markets", John Wiley and Sons, Ltd., Publication
- [2] Brandao, A.F., Jr.; de Silos, A.C.; Ivanoff, D.; da Silva, I.P.; , "A method for field verification of the precision class of inductive voltage transformers," High Voltage Engineering, 1999. Eleventh International Symposium on (Conf. Publ. No. 467) , vol.1, no., pp.209-212 vol.1, 1999
- [3] Mollinger, J & Gewecke, H "Zum Diagramm des Stromwandlers" Elektrotechnische Zeitschrift (V.D.E. -Verlag) vol. 33, 1912, pp 270-271.
- [4] Torre, F.D.; Faifer, M.; Morando, A.P.; Ottoboni, R.; Cherbaucich, C.; Gentili, M.; Mazza, P.; , "Instrument transformers: A different approach to their modeling," Applied Measurements for Power Systems (AMPS), 2011 IEEE International Workshop on , vol., no., pp.37-42, 28-30 Sept. 2011
- [5] Klatt, M.; Meyer, J.; Elst, M.; Schegner, P.; , "Frequency Responses of MV voltage transformers in the range of 50 Hz to 10 kHz," Harmonics and Quality of Power (ICHQP), 2010 14th International Conference on , vol., no., pp.1-6, 26-29 Sept. 2010
- [6] Zhao, S.; Li, H.Y.; Crossley, P.; Ghassemi, F.; , "Testing and modelling of voltage transformer for high order harmonic measurement," Electric Utility Deregulation and Restructuring and Power Technologies (DRPT), 2011 4th International Conference on , vol., no., pp.229-233, 6-9 July 2011
- [7] Kucuksari, S.; Karady, G.G.; , "Experimental Comparison of Conventional and Optical VTs, and Circuit Model for Optical VT," Power Delivery, IEEE Transactions on , vol.26, no.3, pp.1571-1578, July 2011
- [8] EN 60044-2 Instrument transformers - Part 2 : Inductive voltage transformers 03/2003
- [9] Kawamura, K.; Saito, H.; Noto, F.; "Development of a high voltage sensor using a piezoelectric transducer and a strain gage", Instrumentation and Measurement, IEEE Transactions on, Volume: 37 , Issue: 4, Publication Year: 1988 , Page(s): 564 – 568
- [10] Aikawa, E.; Ueda, A.; Watanabe, M.; Takahashi, H.; Imataki, M.; "Development of new concept optical zero-sequence current/voltage transducers for distribution network", IEEE Trans. On Power Delivery, Vol. 6, Issue 1, Jan. 1991 Page(s):414 – 420
- [11] L. H. Christensen, "Design, construction, and test of a passive optical prototype high voltage instrument transformer," IEEE Trans. Power Delivery, vol. 10, pp. 1332–1337, July 1995.
- [12] Fam, W.Z.; "A novel transducer to replace current and voltage transformers in high-voltage measurements", Instrumentation and Measurement, IEEE Transactions on, Volume: 45 , Issue: 1, Publication Year: 1996 , Page(s): 190 – 194
- [13] Cruden, A.; Richardson, Z.J.; McDonald, J.R.; Andonovic, I.; Laycock, W.; Bennett, A.; "Compact 132 kV combined optical voltage and current measurement system" Instrumentation and Measurement, IEEE Transactions on, Volume 47, Issue 1, Feb. 1998 Page(s):219 – 223
- [14] A. Delle Femine, C. Landi, M. Luiso, "Optically Insulated Low Cost Voltage Transducer for Power Quality Analyses", Shaker Verlag Transactions on Systems, Signals and Devices Vol. 4, No. 4, Issues on Sensors, Circuits & Instrumentation, December 2009, ISBN 978-3-8322-8823-5, ISSN 1861-5252
- [15] A. Delle Femine, D. Gallo, C. Landi, M. Luiso, "Broadband Voltage Transducer with Optically Insulated Output for Power Quality Analyses", Proceedings of IEEE Instrumentation and Measurement Technology Conference IMTC 2007, 1-3 May 2007, Warsaw, Poland.
- [16] D. Gallo, C. Landi, M. Luiso, "A Voltage Transducer for Electrical Grid Disturbance Monitoring over a Wide Frequency Range", Proceedings of IEEE International Instrumentation and Measurement Technology Conference I2MTC 2010, Austin, Texas, USA, May 3-6 2010
- [17] D. Gallo, C. Landi, M. Luiso, "Electronic Instrument Transducer for MV Networks with Fiber Optic Insulation", Proceedings of IEEE International Instrumentation and Measurement Technology Conference I2MTC 2011, Binjiang, Hangzhou, China, May 10-12 2011.

- [18] IEC 61936-1 Ed. 2.0, "Power installations exceeding 1 kV a.c. - Part 1: Common rules", 2010-08
- [19] IEC EN 61000-4-30: "Testing and measurement techniques – Power quality measurement methods", 11/2003.
- [20] E. Fiorucci, G. Bucci, F. Ciancetta, "Metrological Characterization of Power Quality Measurement Stations: a Case Study" IJIT International Journal of Instrumentation Technology (IJIT) ISSN: 2043-7862 DOI 10.1504/IJIT.2011.043595
- [21] D. Castaldo, D. Gallo, C. Landi, E. Fiorucci "Measurement Network Infrastructure for Power Quality Monitoring" Shaker Verlag Transactions on Systems, Signals and Devices, volume 1, no. 4, pp. 387-404, 2005-2006. ISSN: 1861-5252
- [22] IEC EN 61000-2-4: "Environment - Compatibility levels in industrial plants for low-frequency conducted disturbances", 04/2003.
- [23] Johnson, Mark; "Photodetection and Measurement - Maximizing Performance in Optical Systems", McGraw-Hill, 2003.
- [24] Khalil, Hassan K.; "Nonlinear systems", (second edition), Prentice Hall, 1996.